Laser based remote and rapid inspection for composite plates

Zhaoyun Ma, Lingyu Yu
Department of Mechanical Engineering, University of South Carolina
Columbia, SC, USA
zhaoyun@email.edu , yu3@cec.sc.edu

ABSTRACT

Composites have been extensively used in aero structure and become the predominate components in the new airframes. Thus, rapid and effective inspection for composite structures is highly desired in aerospace engineering in order to shorten the certificate cycle for new structures or provide safety guarantee for existing ones. In this paper, a laser based remote Lamb wave inspection system is presented and implemented on composite plates for simulated damage detection. The system employs pulsed laser (PL) and scanning laser Doppler vibrometer (SLDV) for noncontact and remote Lamb wave actuation and wavefield sensing. A composite plate with simulated defect (surface bonded quartz rod) is inspected with the PL-SLDV laser system. Wave scattering are observed in the SLDV acquired wavefield and the damage is further evaluated with wavefield imaging and frequency wavenumber analysis. Potential application towards automatic PL Lamb wave excitation is also explored through employing an industry robotic arm towards rapid inspection.

Keywords: Lamb waves, remote inspection, pulsed laser, laser vibrometer, composites, automatic excitation

1 INTRODUCTION

Composite structures are light weight and flexible for engineering design to achieve high strength in the desired dimension. Thus, they have been widely used in aero structures and become the predominate components in the new airframes. For example, composites take up to 50% in the total weight of Boeing 787 Dreamliner airframe. During the manufacturing process, wrinkles and porosity may appear, which may weaken the structure strength and may lead to catastrophic failure in the end. Composite structures may also encounter unexpected impact from bird and debris during their flight service, which may result in matrix cracking and delamination and can directly cause the structure failure. Rapid and effective inspection of composite structures is highly desired in order to shorten the certificate cycle for new structures or provide safety guarantee for existing ones.

Lamb wave based nondestructive evaluation methods have been extensively studied on composite structure inspection and have been proved effective [1-8]. Various transducers have been employed for Lamb wave actuation such as piezoelectric transducers (PZT) [9, 10], pulsed laser (PL) [7, 11], air-coupled transducers (ACT) [12], and electromagnetic transducers (EMAT) [13] while for Lamb wave sensing such as PZT [9], ACT [14], EMAT [13], optic fibers [15], and laser vibrometer [10, 11, 16]. Among them pulsed laser has the advantages of achieving non-contact and remote Lamb wave actuation at a relative far distance and being applicable to extreme conditions such as radiation environments compared to ACT and EMAT. The working principle for lased based Lamb wave generation is based on thermoelastic regime, where the output laser pulse heats the small exciting surface area in a short time so that sudden thermal expansion will be generated, and the recoil effect will result in Lamb wave generation. For Lamb wave remote sensing, scanning Laser Doppler vibrometer (SLDV) has been adopted in Lamb wave applications in recent years since it can measure multidimensional wavefield which contains wealthy information of Lamb wave and wave-damage interaction characteristics [10, 11, 16, 17]. The SLDV measures the surface particle motions along the laser beam based on Doppler frequency or phase shift effect.

In this paper, a laser based noncontact Lamb wave inspection system is developed by combining the pulsed laser for remote Lamb wave actuation and scanning laser Doppler vibrometer (SLDV) for multidimensional Lamb wave wavefield sensing. A composite plate with simulated defect (surface bonded quartz rod) is inspected with 1D and 2D inspection schemes using the presented remote and noncontact PL-SLDV laser system. Strong wave interactions are observed in the acquired wavefield when the incident Lamb waves encounter the simulated damage: most of the waves reflected and some waves by pass the quartz and split to other directions. Multidimensional Fourier analysis is performed, and new wavenumbers are observed. Wavefield imaging is further generated and part of the damage profile is quantified. Potential application towards automatic PL Lamb wave excitation is also explored by employing an industry KUKA arm.

2 PL-SLDV INSPECTION SYSTEM

The PL-SLDV Lamb wave inspection system employs noncontact pulsed laser as actuator to excite Lamb waves in the testing plate through thermoelastic regime and scanning laser Doppler vibrometer for multidimensional time-space Lamb wavefield sensing based on Doppler effect. Traditionally the pulsed laser is placed in a way that the laser beam is perpendicular to the excitation surface. Thus, more thermoelastic expansion of the target area will be achieved resulting in higher strength Lamb wave generation. The SLDV laser head is arranged that the laser beam is also normal to the surface of the inspection area so that only the out-of-plane surface particle motions will be measured. The PL and SLDV can be placed on the same or opposite side of the testing specimen based on inspection requirements.

The noncontact PL-SLDV system experimental setup is shown in Figure 1. A Quantel CFR400 Q-switch pulsed laser with full power 332 mJ is adopted as the Lamb wave actuator. The wavelength of the pulsed laser is 1064 nm, which is in the invisible range. The pulse width is 7 ns and the near field beam diameter is 5.5 mm. The maximum repetition rate of the pulsed laser is 20 Hz. In order to protect the inspecting specimen surface from burning of the pulsed laser excitation, a protective layer is bonded on the specimen surface, which can be easily peeled off after experiment. Polytec PSV-400 SLDV is used as the multidimensional wavefield sensor. In order to improve the SLDV signal quality, reflective tapes are attached on the inspection area on the specimen surface. The PL and SLDV heads are placed on the opposite side of the testing plate and both laser heads are set normal to the specimen in this study. Q-switch box is used to send pulse trains to PL control box at a certain frequency to enable the PL actuation and trigger the SLDV measurement simultaneously.

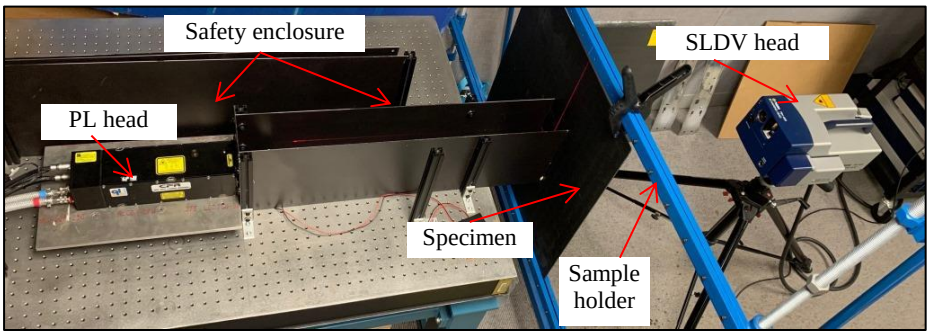

Figure 1 Lased based remote PL-SLDV laser inspection system experimental setup

3 DAMAGE INSPECTION ON AN COMPOSITE PLATE

With the presented PL-SLDV Lamb wave inspection system, a composite plate with simulated damage is inspected and evaluated compared to a pristine plate. The simulated damage is a 10 mm diameter circular quartz rod bonded on the specimen surface. The composite plate is a 8-ply quasi-isotropic plate with layup $[0/45/90/-45]_s$. The dimension of the plate is 610 × 610 × 2.54 (unit: mm). 1D inspection is performed first for a quick Lamb wave characterization as well as to capture the wave damage interaction characteristics. 2D inspection is then further conducted in order to capture more details and quantify the damage. The pulsed laser excitation energy is set as 100 mJ for proof of concept study. The pulsed laser repetition rate is set as 20 kHz.

The inspection actuation and sensing setup is illustrated in Figure 2 with Figure 2a for 1D inspection and Figure 2b for 2D inspection respectively. Cartesian coordinates are used in this study with the origin set at the excitation location. A 0.13 mm thick and 8 mm diameter aluminum foil is attached on the excitation point to protect the surface from burning. The quartz is located at y=70 mm. The scanning line is along y direction (90º fiber direction) from 10 mm to 100 mm for 1D inspection, while the scanning area is about 60 mm by 90 mm for 2D inspection. The SLDV spatial resolution is set as 1 mm for both 1D and 2D inspection. The SLDV sampling rate is set at 10.24 MHz and velocity decoder VD-09 is used which can measure signals up to frequency 1 MHz. Ten averages are used to improve the SLDV signal to noise ratio.

The acquired time-space wavefields of the pristine and damage plate are presented in Figure 3a and Figure 3b respectively. In the pristine plate wavefield, only two incident Lamb wave mode are observed: fast, weak, and nondispersive S_0 while slow, strong, and dispersive A_0. In the damage plate wavefield, S_0 to A_0 mode conversion appeared except the incident waves when waves interacted with the bonded quartz (approximately at y = 65 mm, where the quartz

edge is). In addition, A_0 reflections are observed clearly at the quartz edge. In order to further capture the wave-damage interaction characteristics, 2D Fourier transform [17] is conducted to transfer the time-space wavefield data into frequency and wavenumber domain. The obtained frequency-wavenumber (f-k) spectra are plotted in Figure 3c and Figure 3d respectively, as well as theoretical dispersion curves for comparison purpose. In the f-k spectrum of pristine plate, two positive wave modes are observed which matches theoretical S_0 and A_0 dispersion curves, which confirmed the wave mode characterization in the wavefield. The S_0 mode is weaker and the A_0 mode is significantly stronger, which agrees with the wave phenomena observed in the time-space wavefields. In addition, the A_0 components concentrated on mostly at the low frequency range (lower than 200 kHz). Different from pristine plate, reflected A_0 is observed in addition to the incident S_0 and A_0 modes, indicating that damage may exist in the structure.

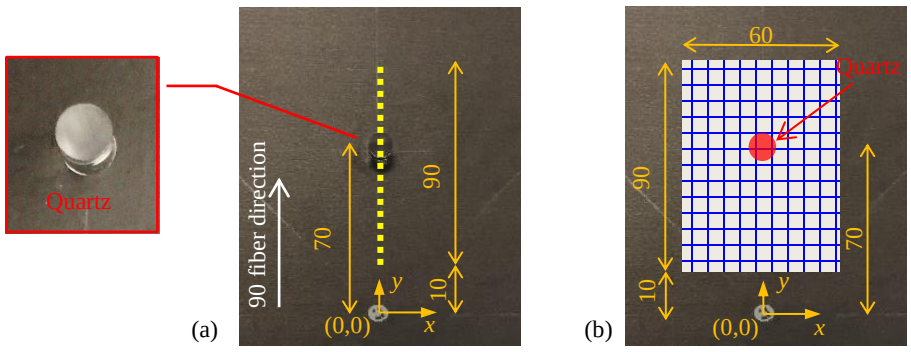

Figure 2 Actuation and sensing schematic: (a) 1D inspection, and (b) 2D inspection

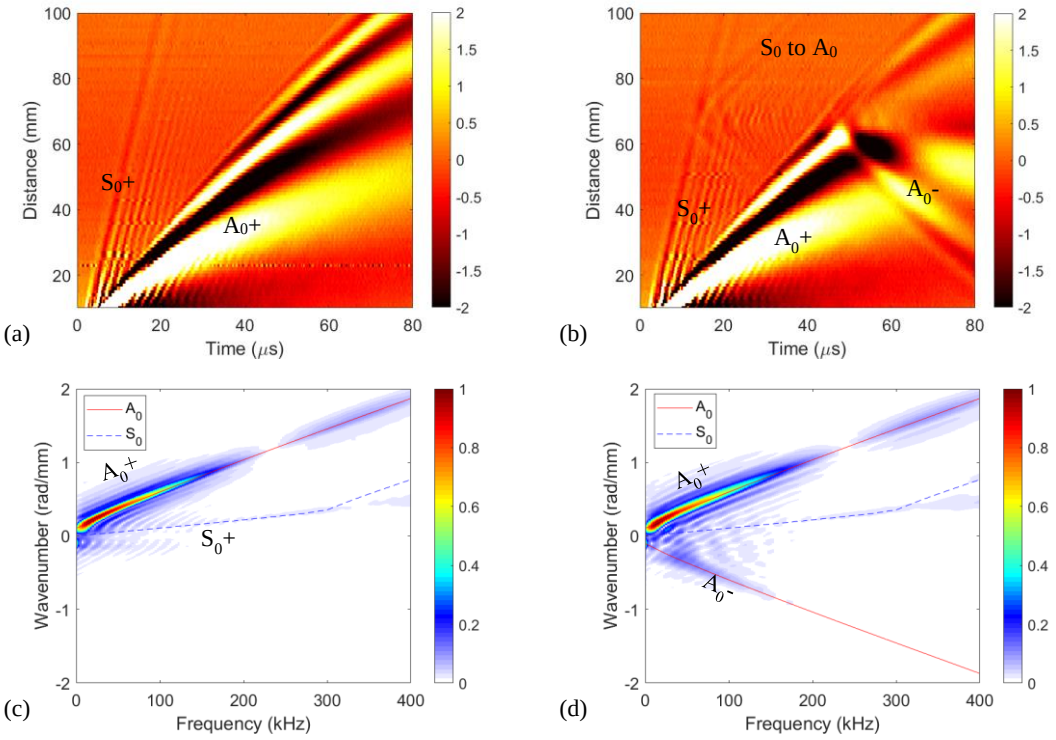

Figure 3 1D inspection results: time-space wavefield of (a) pristine plate, and (b) damage plate; frequency-wavenumber spectrum of (c) pristine plate, and (d) damage plate

In order to capture more details of the wave-damage interaction, 2D inspection is performed. The SLDV acquired time-space wavefields at 60 μs of the pristine plate and damage plate is shown in Figure 4a and Figure 4d respectively to visualize the wave-damage interaction. Compared to the pristine plate, where only incident waves exist, scattered waves are observed when the waves interact with the quartz damage. In addition, the waves are blocked along *y* direction due to the existence of the quartz damage. Energy field images are generated and presented in Figure 4b and Figure 4e by calculating the peak amplitude of each measured waveform at the defined scanning points. The energy field image of pristine plate (Figure 4b) shows that the wave energy attenuates with wave propagation. Note that the red line at about *y*=75 mm is not a damage and it is caused by overlapping of the reflective boundaries, which can be avoided by using wipe-off reflective sprays. For the damage plate, a sharp energy drop is observed at *y*=65 (the quartz edge location) and the wave energy keep decreasing after the quartz, indicating that most of the wave energy is scattered due to the quartz. The bottom part of the quartz profile is indicated as a circular shape which agrees well with the quartz dimension (the white dash circle). Note that the line due to reflective tape overlapping is not showing in Figure 4f since the tape is removed and new tapes are reattached.

The Lamb wave-damage interaction characteristics in the frequency-wavenumber domain is also explored through 3D Fourier transform [17]. The obtained wavenumber spectra at selected frequencies 90 and 150 kHz are presented in Figure 4. In the wavenumber spectrum of pristine plate at both 90 kHz and 150 kHz, incident A0 is observed and agrees well with the theoretical wavenumber curve (red dash line). In the wavenumber spectrum of damage plate, scattered A0 is observed in addition to the incident A0, and some new wavenumbers (lower than A0 wavenumber) are observed for both frequencies. However, the scattered A0 and new wavenumber components are more obvious and stronger at 90 kHz than that at 150 kHz. Thus, 90 kHz is more preferential for further imaging processing such as filtering based imaging or wavenumber imaging.

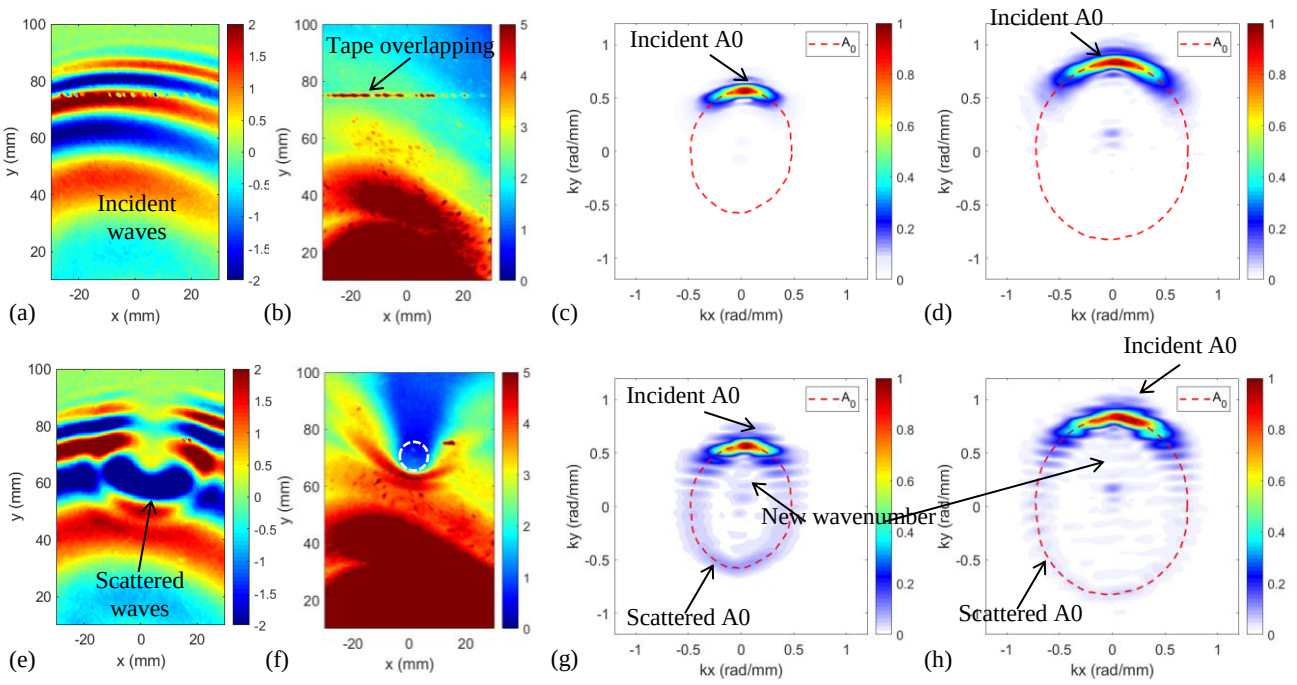

Figure 4 1D inspection results: time-space wavefield of (a) pristine plate, and (e) damage plate; energy field images of (b) pristine plate, and (f) damage plate; wavenumber spectrum at 90 kHz of (c) pristine plate, and (g) damage plate; and wavenumber spectrum at 150 kHz of (d) pristine plate, and (h) damage plate

4 AUTOMATIC PL ACTUATION

The automatic pulsed laser actuation which can excite Lamb waves on any desired location flexibly is explored in this section to enable rapid NDE inspection during manufacturing process of composite structures or any their service time. The PL-SLDV NDE system presented in Section 2, where the PL is fixed on the experiment table, can only excite Lamb waves at a fixed location. Toward automatic PL-SLDV NDE system, the PL head in mounted on an industrial KUKA robotic arm in order to enable the PL excitation movement. The experimental setup of the robotic PL-SLDV NDE system is shown in Figure 5a. KUKA SmartPad (Figure 5b) connected to the KUKA arm is used to enable the PL excitation movement. Since the laser output beam is invisible, two class I line lasers (one is set up as horizontal and the other is vertical w.r.t the laser source) are used for the alignment as shown in as shown in **Error! Reference source not found.**c. An example positioning PL excitation point is illustrated in **Error! Reference source not found.**d. Other settings keep the same as the laboratory PL-SLDV system setup.

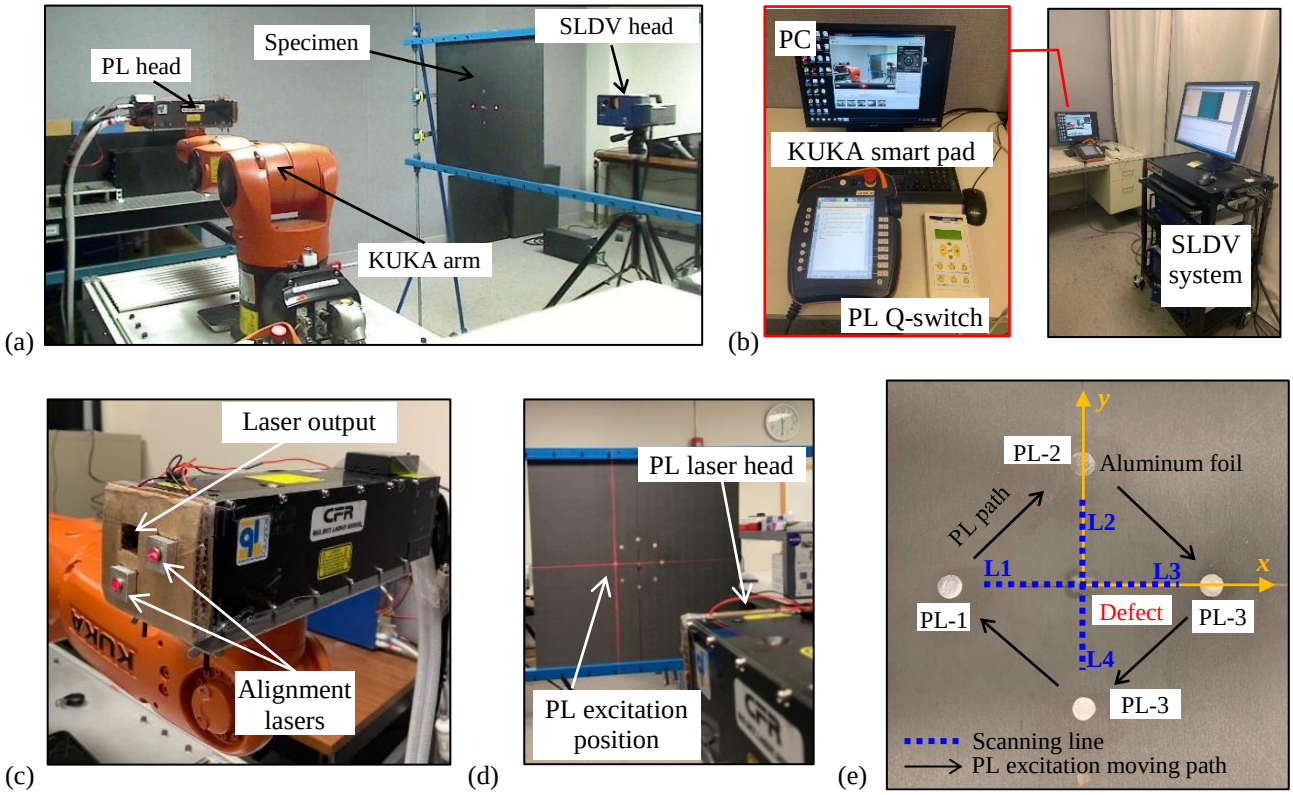

Figure 5 Experimental setup of the robotic PL-SLDV NDE system: (a) PL-specimen-SLDV, (b) PL, SLDV, and KUKA controlling system, (c) Alignment line-lasers mounted on the PL head, (d) Alignment line-lasers positioning the PL excitation point, and (e) 1D inspection actuation and sensing schematic

For proof of concept study, four locations (PL-1, PL-2, PL-3, and PL-4) on a composite plate are selected as target point of PL excitation as shown in Figure 5e. The composite plate has a 10 mm circular quartz bonded as a simulated damage at the center location, which is defined as the origin of the coordinates. With each PL excitation, the SLDV will perform a quick line scan simultaneously from 10 to 100 mm away from the PL excitation point with spatial resolution 0.5 mm. The time-space wavefield acquired by SLDV for the four line-scans with the four different PL excitation locations are plotted in Figure 6. The time-space wavefields obtained at PL-1 and PL-3 are along 0 fiber direction, while those at PL-2 and PL-4 are along 90 fiber direction. The time-space wavefields along L2 and L4 obtained with PL-2 and PL-4 are consistent with that obtained using the fixed PL-SLDV NDE system with line scan also along 90 fiber direction as shown in Figure 3b. The time-space wavefields obtained at PL-1 and PL-3 are slightly different since the line scans are along 0 fiber direction. Mode conversion S_0 to A_0 and A_0 reflections are observed in all wavefields at 65 mm away from the excitation

location where the quartz edge is when the waves interact with the defect. With the automatic PL-SLDV system, valid wavefields are measured and effective inspection purpose is achieved.

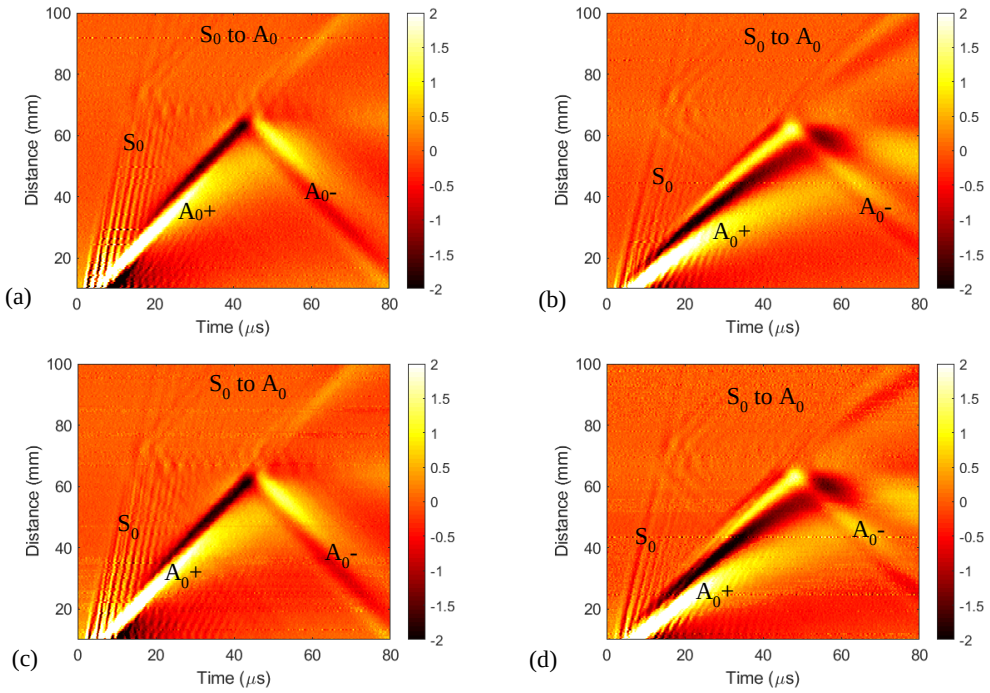

Figure 6 Time-space wavefield results of the 1D inspection with automatic PL excitation at: (a) PL-1, (b) PL-2, (c) PL-3, and (d) PL-4, showing that the wavefield results are consistent with those obtained by fixed PL-SLDV NDE system

5 CONCLUSIONS

In this paper, a laser based Lamb wave PL-SLDV inspection system is presented to enable remote and rapid NDE inspection composite plates. The PL-SLDV system employs pulsed laser for remote Lamb wave actuation through thermoelastic regime and scanning laser Doppler vibrometer for wavefield sensing based on Doppler effect. A composite plate with simulated defect is inspected compared to a pristine plate using the presented remote and noncontact PL-SLDV laser system. Two fundamental Lamb wave modes S_0 and A_0 are excited in the tested plate. S_0 to A_0 Mode conversion and A_0 wave scattering are observed when the incident Lamb waves encounter the simulated damage in the wavefields. Scattered A_0 is also observed in the wavenumber spectrum and new wavenumbers are observed in addition to the excited A_0. Part of the damage profile is quantified through wavefield imaging method. Potential application towards automatic PL Lamb wave excitation is also explored by employing an industry KUKA arm. The results showing consist results with that acquired with the fixed PL-SLDV system. Future work can be focused on development of other imaging algorithms to quantify the damage profile and application of the PL-SLDV system on inspection composite plates with typical defects and damage such as wrinkles and delamination. In addition, the further exploration of the automatic PL-SLDV system on effective damage inspection on composite plates is also recommended.

6 ACKNOWLEDGEMENT

The material is based upon work supported by NASA under Award Nos. NNL09AA00A and 80LARC17C0004. Any opinions, findings, and conclusions or recommendations expressed in this material are those of the author(s) and do not necessarily reflect the views of the National Aeronautics and Space Administration.

7 REFERENCES

[1] H. W. Park, H. Sohn, K. H. Law *et al.*, "Time reversal active sensing for health monitoring of a composite plate," Journal of Sound and Vibration, 302(1-2), 50-66 (2007).

[2] A. Purekar, and D. Pines, "Damage detection in thin composite laminates using piezoelectric phased sensor arrays and guided Lamb wave interrogation," Journal of Intelligent Material Systems and Structures, 21(10), 995-1010 (2010).

[3] C. Garnier, M.-L. Pastor, F. Eyma *et al.*, "The detection of aeronautical defects in situ on composite structures using Non Destructive Testing," Composite Structures, 93(5), 1328-1336 (2011).

[4] H. Sohn, D. Dutta, J.-Y. Yang *et al.*, "Delamination detection in composites through guided wave field image processing," Composites science and technology, 71(9), 1250-1256 (2011).

[5] K. E. Cramer, C. A. Leckey, P. A. Howell *et al.*, "Quantitative NDE of Composite Structures at NASA," (2015).

[6] Z. Tian, L. Yu, and C. Leckey, "Delamination detection and quantification on laminated composite structures with Lamb waves and wavenumber analysis," Journal of Intelligent Material Systems and Structures, 26(13), 1723-1738 (2015).

[7] Z. Tian, S. Howden, Z. Ma *et al.*, "Pulsed laser-scanning laser Doppler vibrometer (PL-SLDV) phased arrays for damage detection in aluminum plates," Mechanical Systems and Signal Processing, 121, 158-170 (2019).

[8] L. Yu, Z. Tian, X. Li *et al.*, "Core–skin debonding detection in honeycomb sandwich structures through guided wave wavefield analysis," Journal of Intelligent Material Systems and Structures, 30(9), 1306-1317 (2019).

[9] V. Giurgiutiu, [Structural health monitoring: with piezoelectric wafer active sensors] Elsevier, (2007).

[10] L. Yu, and Z. Tian, "Lamb wave structural health monitoring using a hybrid PZT-laser vibrometer approach," Structural Health Monitoring, 12(5-6), 469-483 (2013).

[11] Y.-K. An, B. Park, and H. Sohn, "Complete noncontact laser ultrasonic imaging for automated crack visualization in a plate," Smart Materials and Structures, 22(2), (2013).

[12] M. Castaings, and P. Cawley, "The generation, propagation, and detection of Lamb waves in plates using air‐coupled ultrasonic transducers," The Journal of the Acoustical Society of America, 100(5), 3070-3077 (1996).

[13] P. D. Wilcox, M. J. Lowe, and P. Cawley, "The excitation and detection of lamb waves with planar coil electromagnetic acoustic transducers," IEEE Transactions on ultrasonics, ferroelectrics, and frequency control, 52(12), 2370-2383 (2005).

[14] M. S. Harb, and F.-G. Yuan, "Damage imaging using non-contact air-coupled transducer/laser Doppler vibrometer system," Structural Health Monitoring, 15(2), 193-203 (2016).

[15] F. Li, H. Murayama, K. Kageyama *et al.*, "Guided wave and damage detection in composite laminates using different fiber optic sensors," Sensors, 9(5), 4005-4021 (2009).

[16] H. Sohn, D. Dutta, J. Yang *et al.*, "Automated detection of delamination and disbond from wavefield images obtained using a scanning laser vibrometer," Smart Materials and Structures, 20(4), 045017 (2011).

[17] Z. Ma, and L. Yu, "Lamb wave defect detection and evaluation using a fully non-contact laser system." 10972, 1097221.